Konrad-Zuse-Zentrum
für Informationstechnik Berlin

Takustraße 7
D-14195 Berlin-Dahlem
Germany

MARTIN HAMMERSCHMIDT, DANIEL LOCKAU, LIN ZSCHIEDRICH, FRANK SCHMIDT

Optical modelling of incoherent substrate light-trapping in silicon thin film multi-junction solar cells with finite elements and domain decomposition

This paper is made available as an electronic preprint with permission of SPIE and will be published in Proc. SPIE 8980, 898007 (2014). The full citation reads:
Martin Hammerschmidt, Daniel Lockau, Lin Zschiedrich and Frank Schmidt, "Optical modelling of incoherent substrate light-trapping in silicon thin film multi-junction solar cells with finite elements and domain decomposition", Physics and Simulation of Optoelectronic Devices XXII, Bernd Witzigmann, Marek Osinski, Fritz Henneberger, Yasuhiko Arakawa, Editors, Proc. SPIE 8980, 898007 (2014).

http://dx.doi.org/10.1117/12.2036346

Herausgegeben vom
Konrad-Zuse-Zentrum für Informationstechnik Berlin
Takustraße 7
D-14195 Berlin-Dahlem

Telefon: 030-84185-0
Telefax: 030-84185-125

e-mail: bibliothek@zib.de
URL: http://www.zib.de

ZIB-Report (Print) ISSN 1438-0064
ZIB-Report (Internet) ISSN 2192-7782

Optical modelling of incoherent substrate light-trapping in silicon thin film multi-junction solar cells with finite elements and domain decomposition

Martin Hammerschmidt[a], Daniel Lockau[a,b], Lin Zschiedrich[a,c], Frank Schmidt[a,c]

[a]Konrad-Zuse-Zentrum für Informationstechnik Berlin, Takustraße 7, 14195 Berlin, Germany
[b]Helmholtzzentrum für Materialien und Energie, Kekuléstraße 5, 12489 Berlin , Germany
[c]JCMwave GmbH, Bolivarallee 22, 14050 Berlin, Germany

This paper is made available as an electronic preprint with permission of SPIE and will be published in Proc. SPIE 8980, 898007 (2014). The full citation reads:
Martin Hammerschmidt, Daniel Lockau, Lin Zschiedrich and Frank Schmidt, "Optical modelling of incoherent substrate light-trapping in silicon thin film multi-junction solar cells with finite elements and domain decomposition", Physics and Simulation of Optoelectronic Devices XXII, Bernd Witzigmann, Marek Osinski, Fritz Henneberger, Yasuhiko Arakawa, Editors, Proc. SPIE 8980, 898007 (2014).

http://dx.doi.org/10.1117/12.2036346

ABSTRACT

In many experimentally realized applications, e.g. photonic crystals, solar cells and light-emitting diodes, nanophotonic systems are coupled to a thick substrate layer, which in certain cases has to be included as a part of the optical system. The finite element method (FEM) yields rigorous, high accuracy solutions of full 3D vectorial Maxwell's equations[1] and allows for great flexibility and accuracy in the geometrical modelling. Time-harmonic FEM solvers have been combined with Fourier methods in domain decomposition algorithms to compute coherent solutions of these coupled system.[2,3] The basic idea of a domain decomposition approach lies in a decomposition of the domain into smaller subdomains, separate calculations of the solutions and coupling of these solutions on adjacent subdomains. In experiments light sources are often not perfectly monochromatic and hence a comparision to simulation results might only be justified if the simulation results, which include interference patterns in the substrate, are spectrally averaged. In this contribution we present a scattering matrix domain decomposition algorithm for Maxwell's equations based on FEM. We study its convergence and advantages in the context of optical simulations of silicon thin film multi-junction solar cells. This allows for substrate light-trapping to be included in optical simulations and leads to a more realistic estimation of light path enhancement factors in thin-film devices near the band edge.

Keywords: finite element method, rigorous optical modeling, domain decomposition, multi-junction solar cells, thin-film silicon solar cells, incoherent layers, incoherent light-trapping

1. INTRODUCTION AND PROBLEM SETTING

In many experimentally realized applications, e.g. photonic crystals, solar cells and light-emitting diodes, nanophotonic systems are coupled to a thick substrate layer, which in certain cases has to be included as a part of the optical system. In many of these, a glass layer of several mm thickness is used as a substrate and is commonly treated as an incoherent layer that does not show interference effects in reflection or transmission measurements and removes phase correlations between the illumination and the transmitted light. There have been several models employing coherent and incoherent light propagation presented within the literature in

Further author information: (Send correspondence to Martin Hammerschmidt)
Martin Hammerschmidt: E-mail: hammerschmidt@zib.de, Telephone: +49 30 84185-149

the proceeding years. They offer models for very specific problem classes such as multilayer systems[4] and randomly textured thin-film solar cells in combination with the scalar scattering theory.[5,6] These cases are not applicable to general 3D scattering problems. The required averaging over a reasonably large ensemble of statistical parameter fluctuations in the so called incoherent layers is usually omitted in models of more complex 2D and 3D structures. Instead, reduced[7] or iterative[8] models are employed or the results are spectrally averaged. Furthermore, experimental light sources are often not perfectly monochromatic, but rather have a spectral bandwidth even if passed through a monochromator. Models employing partial coherence or incoherent light sources available in literature[9,10] are spectrally averaging the results of several monochromatic simulations as well. For example, the incoherent illumination model presented by Sarrazin et al.[9] uses a convolution of the coherent absorptance spectrum with an incoherence function that depends on frequency and coherence time of the modeled incoherent source. This convolution acts as a parameter dependent moving average filter.

In this work, we focus primarily on the common problem setting in thin-film silicon photovoltaics where the solar cell is illuminated either through the glass substrate or a glass encapsulation. These layers are usually a few mm thick, whereas the complete solar cell measures only a few µ at most. In addition the scattering structures or textures contain subwavelength sized features. This poses a challenge to rigorous simulation routines due to the large discrepency in scale between the glass layer and the solar cell. In most cases the glass layer is not accounted for and the illumination is modeled as incident from a glass half space with a correction for the initial reflection at the air/glass interface using Fresnel's equations. In publications where the glass layer is included, it is usually reduced in thickness and treated coherently.[7] However, this is a physically different problem which may distort interference patterns introduced between a reflector and the glass layer.

2. NUMERICAL METHODS AND SIMULATION ALGORITHMS

2.1 The Finite Element Method

We give a short introduction to the finite element method (FEM) and scattering problem formulations. A more rigorous mathematical formulation of scattering problems with a detailed discussion of the arising boundary conditions than present in the following can be found in.[11]

The linear Maxwell's equations model light scattering off nanoscaled scattering structures located within thin-film solar cells in the frequency domain. These can be reformulated into the following second order curl-curl-equation for the electric field if no embedded sources are present:

$$\nabla \times \mu^{-1} \nabla \times \mathbf{E}(\mathbf{r}) - \omega^2 \varepsilon \mathbf{E}(\mathbf{r}) = 0 \tag{1}$$

where μ and ε are the permeability and permittivity tensors and ω is the time-harmonic frequency of the electromagnetic field.

In scattering problems we investigate light scattering off a scatterer located within a computational domain Ω_{int} that is surrounded by an infinite exterior domain Ω_{ext}. The linearity of Maxwell's equations allows the splitting of the sought after electric field $\mathbf{E}$ into $\mathbf{E}_{in}$ and $\mathbf{E}_{sc}$. Illuminating or incoming electromagnetic fields $\mathbf{E}_{in}$ solve (1) in Ω_{ext}. The scattered field $\mathbf{E}_{sc}$ satisfies (1) in Ω_{in} and is strictly outward radiating. The electric field $\mathbf{E}$ satisfies (1) in Ω_{in} with the continuity boundary condition

$$\mathbf{n} \times (\mathbf{E}_{in} + \mathbf{E}_{sc} - \mathbf{E})\,|_{\Gamma} = 0 \tag{2}$$

on the boundary of Ω_{int} called Γ. In (2) it is observable that the incoming field enters the computation on Ω_{int} via the continuity condition stated on the boundary Γ. In order to discretize (1) with finite elements a weak formulation of (1) on Ω_{int} is employed and the infinite exterior is Ω_{ext} is treated with a transparent boundary condition (in this case the perfectly matched layer method or PML). This yields a linear system

$$\mathcal{A}\mathbf{E}_h = \mathbf{b} \tag{3}$$

where $\mathcal{A}$ is a sparse matrix, $\mathbf{b}$ contains boundary terms like source terms and $\mathbf{E}_h$ holds the coeffients of the electric field solution in the FEM basis which is computed as the inversion of (3) as

$$\mathbf{E}_h = \mathcal{A}^{-1}\mathbf{b}. \tag{4}$$

Note that different sources enter only the right hand side vector $\mathbf{b}$ containing the boundary terms in (3) given that $\mathcal{A}$ does not change. This allows the computation of (4) for different $\mathbf{b}$ at low computational expense as the computationally expensive step is the inversion of $\mathcal{A}$. A trivial example for a problem where $\mathcal{A}$ does not change is the computation of two polarizations in a full 3D vectorial Maxwell problem.

Time-harmonic methods like the FEM solver JCMsuite[1] by JCMwave allow for the direct use of optical material properties without any fitting of the complex refractive index. Furthermore the FEM allows for great geometric flexibility, i.e. variable mesh element sizes to resolve arbitrarily shaped material interfaces with sharp edges and offers higher order finite elements. All computations in the following sections made use of tetrahedral or triangular meshes (in 3D and 2D) whose edge lengths are constrained by at most the wavelength inside the material and a polynomial degree p of at least 3 which has been shown previously to yield reasonable accuracies for this particular model problem. The solver has also been successfully employed in other solar cell simulation studies with high demands for accuracy.[12,13]

2.2 Incoherent Substrate Light Trapping

We will outline the algorithm used for the incoherent substrate light trapping here only briefly. Similar to Campa et al.,[7] we combine several simulations computed for different thicknesses d'_S of the substrate. Computing several solutions with different thicknesses of the substrate results in large computational costs if simulated consecutively. In general, this is infeasible for the problems under consideration, since each individual 3D FEM simulation can be very time-consuming. Campa et al. averaged just two simulations, in which they corrected the substrate thickness to eliminate a phase shift of the specular wave and scaled the glass layer thickness to a micrometers instead of mm to reduce computational costs. We do not use such a scaling of the glass layer thickness in our simulations and keep the mm scale. Instead, we vary the glass layer thickness with the transformation $d'_S = d_S \frac{\lambda_i}{\lambda_0}$ for $\lambda_i \in \lambda_0 + [-1\,\mathrm{nm}, 1\,\mathrm{nm}]$ around the simulated wavelength λ_0 and include the very large, homogeneous subdomain into the computational domain in which the solution to Maxwell's equations is sought. Time-harmonic FEM solvers have been combined with Fourier methods in domain decomposition algorithms to compute coherent solutions of such systems.[2,3] The basic idea of such a domain decomposition approach lies in a decomposition of the domain into smaller subdomains, separate calculations of the solutions and coupling of these solutions on adjacent subdomains in an iterative procedure. Instead of an iterative algorithm, the algorithm presented here uses a tailored scattering matrix domain decomposition strategy. This allows the derivation of a reduced model in which the parameters of the substrate can be varied fast and easily. This is done by computing a scattering matrix for the solar cell domain which can be done efficiently in a periodic setting with FEM solvers (cf. section 2.1). The substrate is treated with semianalytical methods which allows a sequence of solutions for different substrate parameters to be quickly obtained. These electromagnetic field solutions in the FEM domain are summed up coherently and the derived quantities such as absorption and reflection are computed from this superposition. Note that we use a volume integration of the electromagnetic field energy density to compute absorption which generally makes this post processing step of the solution expensive for large computational domains. The use of surface integration is more efficient, but comes at a loss in precision. The number of the volume integration post process evaluations would increase linearly with every substrate thickness point sampled and quadratic if overlap integrals between simulations are taken into account. We exploit the algebraic structure of this post processing step to drastically reduce the number of post processes needed from N^2 to $\leq N$ for N sampling points without loss of accuracy. Details of the mathematical and implementation challenges will be published elsewhere.

3. RESULTS AND DISCUSSION OF TWO MODEL PROBLEMS

3.1 Small Scale Model Problem - Sinusoidal Grating

We test the algorithm on a small scale problem first. The model is a periodic sinusoidal grating structure with a 2 µm period and a 300 nm amplitude. The geometry and the employed triangular finite element mesh in Figure 2 resemble a silicon grating on a textured glass substrate in air. The glass domain (blue) at the bottom is extended with a 1 mm substrate and a second air half space. The reflectivity of the grating at s-polarized illumination of 800 nm vaccuum wavelength from the top is shown on the right at wavelengths between 799 nm and 801 nm. The results of the incoherent light trapping, presented in Figure 3, demonstrate a good convergence of the relative

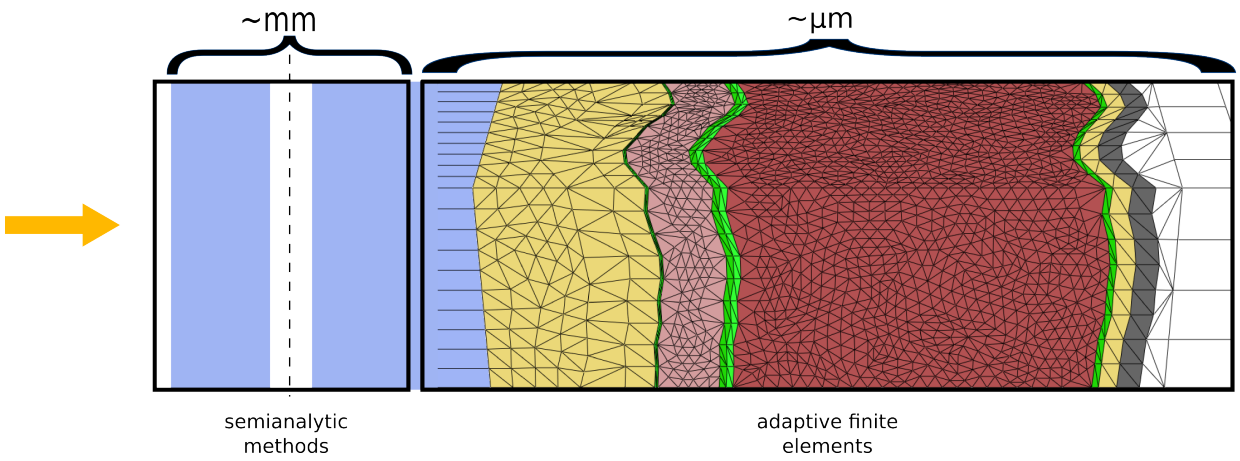

Figure 1. Tailored Domain Decomposition: The two computational domains are indicated by rectangles. A thin-film silicon solar cell with a complex geometry is discretized with adaptive finite elements. The much larger homogeneous area is treated semi-analytically. The direct of incoming light is indicated with an arrow.

error to the mean reflectivity of the reference solution in Figure 2, provided the finite element solution is itself reasonably well converged ($p = 6, 7$. Otherwise the relative error does not depend on the number of sampling points and remains at a fixed error level ($p = 1, 2, 3, 4$) which depends on the accuracy of the finite element solution. To reach a relative accuracy of the incoherent estimate of 1% at least $p = 5$ should be employed for this model problem. Instead of evaluating 201 post process for the reference solution, the estimates presented here were computed with at most 8 post processes. The graph on the right in Figure 3 shows, that the required number of post process evaluations does not increase, if the number of sampling points is increased from 25 to 201. This number is in fact reduced with increased polynomial degree p from 8 to 5.

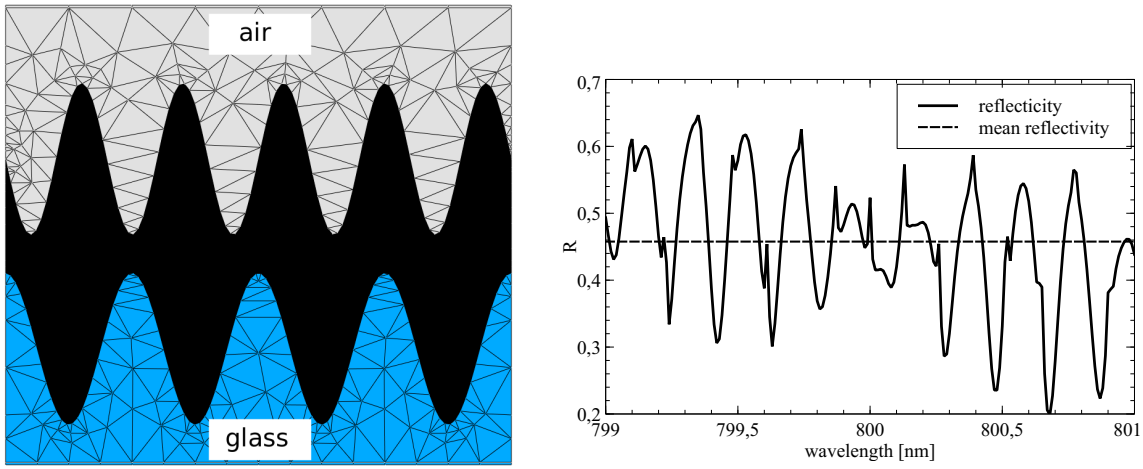

Figure 2. *Left*: Geometry and triangular finite element mesh of a periodic sinusoidal grating structure in silicon with a 2 µm period and a 300 nm amplitude. The three materials are assumed to have refractive indices $n = 1$ (air), $n = 3.5 + i \cdot 10^{-5}$ (silicon) and $n = 1.52$ (glass). *Right*: Reflectivity of the structure shown on the left between 799 nm and 801 nm.

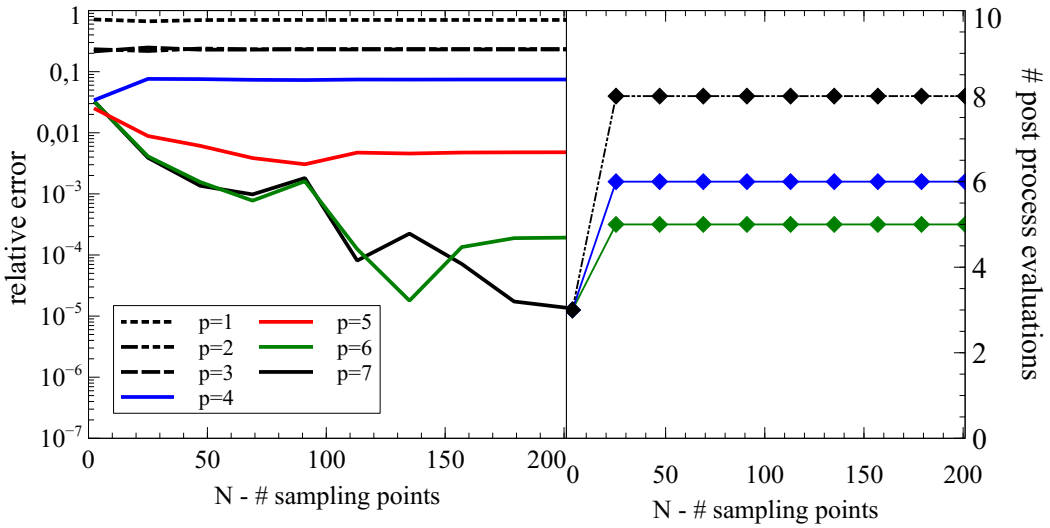

Figure 3. *Left:*Relative error of the incoherent light trapping with the number of equidistant sampling points for simulations of varying finite element degree p compared to the mean reflectance of the reference solution computed for $p = 6$. *Right:* Number of post process evaluations required for $p = 2, 4, 6$.

3.2 Large Scale Model Problem - Textured Thin-film Silicon Tandem Solar Cell

We use the same $1\mu m \times 1\mu m$ xy-axis aligned unit cell presented in[14] as a thin-film silicon tandem solar cell model problem. This particular cell was studied in the cited reference in great detail. We shortly summarize the most important parameters used for this model. The vertical solar cell layer stack contains thick absorber layers (730 nm SnO_2:F, 270 nm a-Si ,1600 nm µc-Si layer and 200 nm silver) as well as thin doped layers (two p-type a-Si layers of 5 nm, 30 nm of n-type a-Si, 30 nm of p- and n-type µc-Si each and a 80 nm ZnO layer), each of them separated by the same synthetic textured interface generated with the autocorrelation data based random texture generation procedure described in the reference.[14] In x- and y-directions periodic boundary conditions are applied. Transparent boundary conditions in $\pm z$ directions are applied, using adaptive perfectly matched layers.[15] Plane waves in $-z$ direction are used as incident fields. The model cell is a a-Si/µc-Si thin-film silicon tandem solar cell in superstrate configuration, i.e. it is illuminated through its glass substrate of several mm thickness. In[14] the contribution of light trapped between the solar cell back reflector and the substrate/air interface on the illumination side has not been taken into account. The glass substrate was modeled as a glass half-space and calculations were corrected with the Fresnel coeffient of the air/substrate interface.

Figure 4 shows a sample finite element grid together with the electric field intensity at 600 nm illumination wavelength. The electromagnetic field is logarithmically scaled and shown as slices in the x-z- and y-z-plane. The bottom cell mesh is omitted for visualization purposes. The right graph in Figure 4 shows the generation rate of both subcells combined between 600 and 1100 nm (black line). In addition, 5 additional plots of the same data are shown, each labeled with the according coherence times (5 fs - 200 fs). These are generated from the coherent data with a parameter dependent, gaussian moving average filter identical to the convolution with the incoherence function presented for the illumination model presented by Sarrazin et al.[9] The chosen coherence times were taken from this reference. Coherence times smaller than 90 fs distort the profile visibly. The spectral averaging with the 200fs filter is roughly equivalent to gaussian filter with a few nm bandwidth and agrees in its shape approximately with the profiles in Figure 5 (iv) and (vi) which were generated by the applying the simple moving average filter.

In Figure 5 the absorptance of all tandem cell layers is shown in the form of area plots, together with the reflectance (shaded area). In subplot (i), the results of Fresnel corrected coherent simulations are shown, not taking the light trapping in the encapsulating glass layer into account. The sampling rate was 5 nm and the relative error in volume absorption was kept below 1%. The inclusion of all doped layers in combination with a low scattering efficiency of the relatively smooth texture lead to many narrow width interference fringes in the

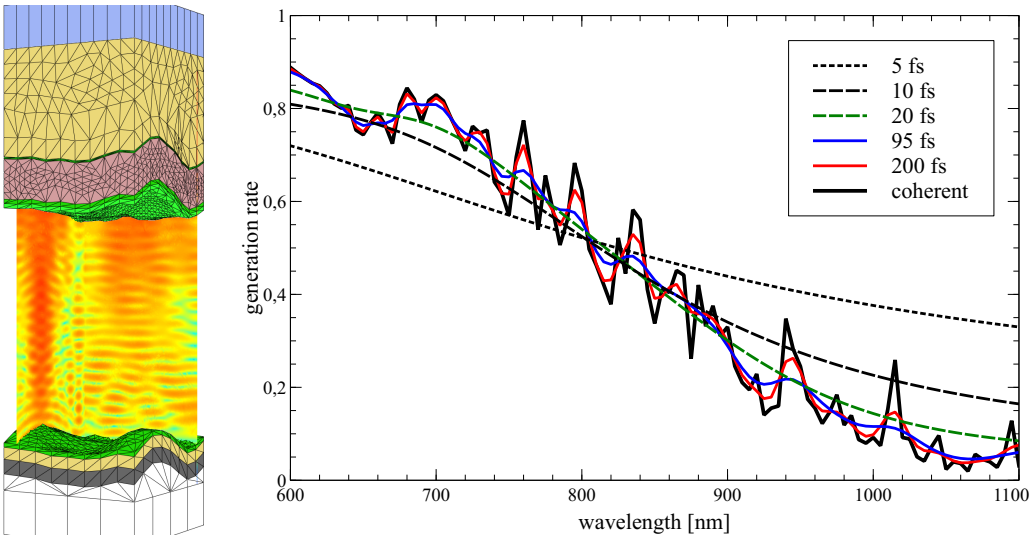

Figure 4. *Left*: Finite element grid of an a-Si/μc-Si tandem solar cell with electric field intensity in the x-z- and y-z-plane on a logarithmic scale at 600 nm wavelength obtained as a solution of Maxwell's equations with periodic boundary conditions applied to lateral boundaries and perfectly matched layer boundary conditions applied to top and bottom boundaries. Light is incident from the top. *Right*: The combined absorptance of both top and bottom cell (black line) is plotted together with moving average filtered versions of the same profile according to different coherence times (5 fs - 200 fs).

total absorptance (1-R). The same data is shown in (ii) with a simple moving average (MA) filter of order 5 applied. The simulation presented in (iii) includes the substrate in a coherent simulation leading to much more pronounced, narrow width interference fringes. For this simulation the wavelength sampling grid (the same as in (i)) is too coarse to resolve the fringes accurately. This simulation is again presented in (iv) with the moving average filter applied. The same simulation with the incoherent superstrate light trapping (shown in (v) and MA filtered in (vi)) has broader and less pronounced fringes. The inclusion of the superstrate yields a reduced reflectance best observed in both (iv) and (vi). The bottom cell absorption is improved as well. When comparing subplots (iv) and (vi), we observe that the local maxima appearing in total absorptance at 1040 nm and 1080 nm are broader and slightly shifted in the incoherent case.

4. CONCLUSION

In this contribution we demonstrated a scattering matrix domain decomposition algorithm that allows not only to include thick substrate layers into the computational domain, but also the computation of a sequence of solutions for different layer thicknesses rapidly. The superposition of these solutions allows the reduction of the effect of dense interference patterns introduced into the simulations by a mm thick homogeneous glass layer. The inclusion of the glass layer is of great importance as it provides a means to estimate cell absorptance more realistically by accounting for light trapped by total internal reflection in the solar cell.

ACKNOWLEDGMENTS

This work was supported by Masdar PV GmbH and the German Federal Ministry for Environment, Nature Conservation and Nuclear Safety (BMU) in the framework of the program "Design und Demonstration der Technologie für Silizium-Dünnschichtsolarzellen mit 14% Zell- und 13% stabilem Modulwirkungsgrad (Demo 14)" as well as the DFG Research Center MATHEON "Mathematics for key technologies" in Berlin. The authors thank J.Pomplun and S.Burger for many useful discussions concerning finite element based modeling and their continued support.

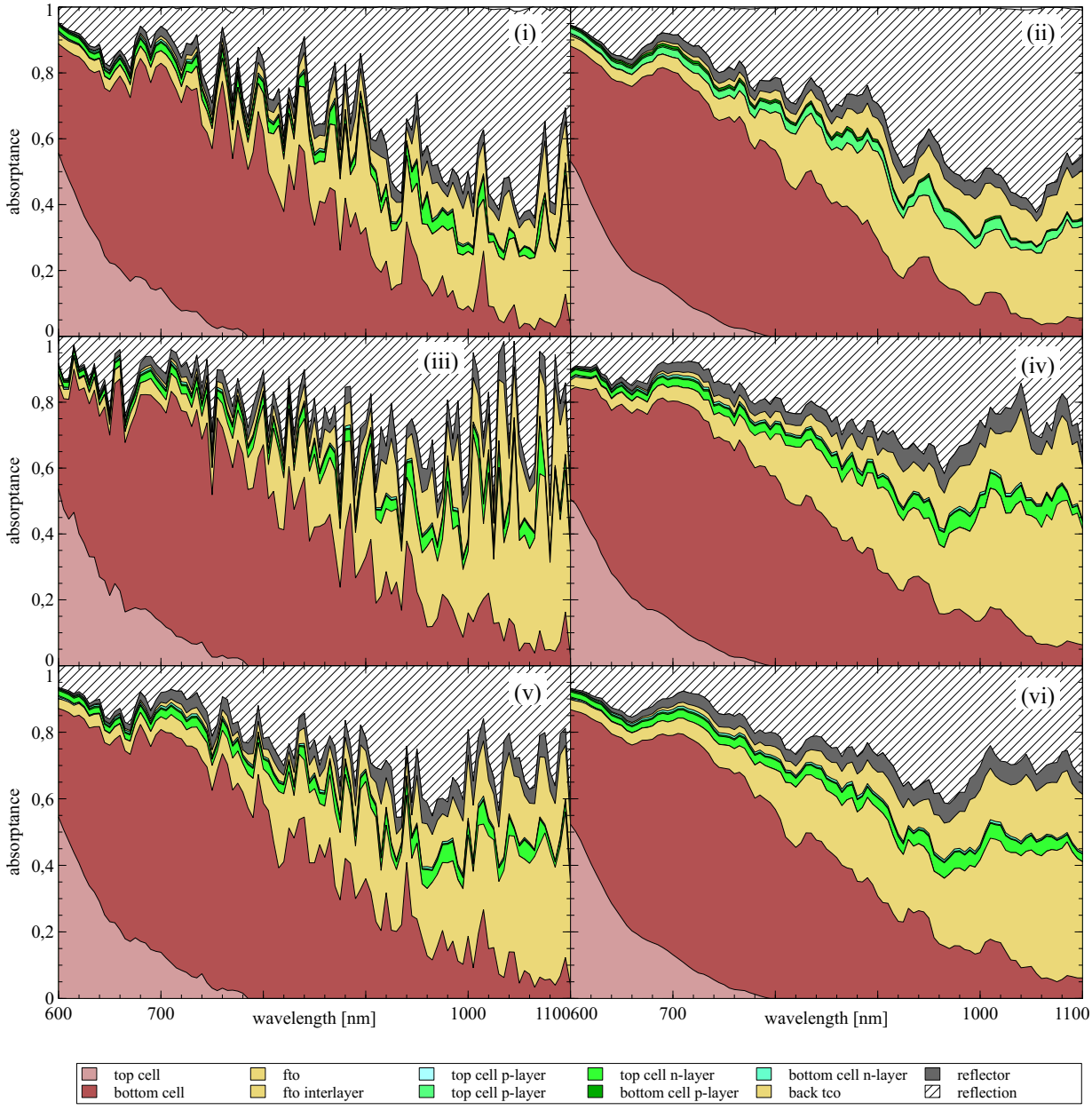

Figure 5. Absorptance plots for the tandem cell in Figure 4. *Left column:* In (i) the coherent simulation is shown without light trapping in the encapsulating glass layer and a fresnel correction instead. The simulation data in (iii) includes the substrate in a coherent simulation leading to much more pronounced narrow width interference fringes. The simulation with the incoherent light trapping in the encapsulating glass layer shown in (v) has broader and less pronounced fringes. *Right column:* The same data as in the left column is plotted with a moving average (MA) filter applied. The inclusion of the glass layer yields a reduced reflectance in both (iv) and (vi) compared to (ii). The bottom cell absorption is improved as well. In contrast to (iv), in (vi) the local maxima in the total absorptance at 1040 nm and 1080 nm are broader and slightly shifted.

REFERENCES

[1] Burger, S., Zschiedrich, L., Pomplun, J., and Schmidt, F., "Jcmsuite: An adaptive fem solver or precise simulations in nano-optics," in [*Integrated Photonics and Nanophotonics Research and Applications*], *Integrated Photonics and Nanophotonics Research and Applications* , ITuE4, Optical Society of America (2008).

[2] Burger, S., Zschiedrich, L., Pomplun, J., Schmidt, F., Kato, A., Laubis, C., and Scholze, F., "Investigation of 3d patterns on euv masks by means of scatterometry and comparison to numerical simulations," *Proc. SPIE* **8166**, 81661Q–81661Q–8 (2011).

[3] Schädle, A., Zschiedrich, L., Burger, S., Klose, R., and Schmidt, F., "Domain decomposition method for maxwells equations: Scattering off periodic structures," *Journal of Computational Physics* **226**(1), 477–493 (2007).

[4] Harbecke, B., "Coherent and Incoherent Reflection and Transmission of Multilayer Structures," *Applied Physics B* **39**, 165–170 (1986).

[5] Krč, J., Smole, F., and Topič, M., "Analysis of light scattering in amorphous si: H solar cells by a one-dimensional semi-coherent optical model," *Progress in photovoltaics: Research and Applications* **11**(1), 1526 (2003).

[6] Santbergen, R., Smets, A. H., Zeman, M., et al., "Optical model for multilayer structures with coherent, partly coherent and incoherent layers," *Opt. Express21, A262–A267* (2013).

[7] Campa, A., Krc, J., et al., "Two approaches for incoherent propagation of light in rigorous numerical simulations," *Progress In Electromagnetics Research* **137**, 187–202 (2013).

[8] Abass, A., Trompoukis, C., Leyre, S., Burgelman, M., and Maes, B., "Modeling combined coherent and incoherent scattering structures for light trapping in solar cells," *Journal of Applied Physics* **114**(3), 033101–033101 (2013).

[9] Sarrazin, M., Herman, A., and Deparis, O., "First-principle calculation of solar cell efficiency under incoherent illumination," *Opt. Express* **21**, A616–A630 (Jul 2013).

[10] Lee, W., Lee, S.-Y., Kim, J., Kim, S. C., and Lee, B., "A numerical analysis of the effect of partially-coherent light in photovoltaic devices considering coherence length," *Opt. Express* **20**, A941–A953 (Nov 2012).

[11] Pomplun, J., Burger, S., Zschiedrich, L., and Schmidt, F., "Adaptive finite element method for simulation of optical nano structures," *phys. stat. sol. (b)* **244**, 3419 – 3434 (2007).

[12] Paetzold, U., Moulin, E., Michaelis, D., Bottler, W., Wachter, C., Hagemann, V., Meier, M., Carius, R., and Rau, U., "Plasmonic reflection grating back contacts for microcrystalline silicon solar cells," *Applied Physics Letters* **99**(18), 181105–181105 (2011).

[13] Becker, C., Lockau, D., Sontheimer, T., Schubert-Bischoff, P., Rudigier-Voigt, E., Bockmeyer, M., Schmidt, F., and Rech, B., "Large-area 2d periodic crystalline silicon nanodome arrays on nanoimprinted glass exhibiting photonic band structure effects," *Nanotechnology* **23**, 135302 (2012).

[14] Hammerschmidt, M., Lockau, D., Burger, S., Schmidt, F., Schwanke, C., Kirner, S., Calnan, S., Stannowski, B., and Rech, B., "FEM-based optical modeling of silicon thin-film tandem solar cells with randomly textured interfaces in 3D," in [*Proc. SPIE 8620, Physics, Simulation, and Photonic Engineering of Photovoltaic Devices II*], 86201H (2013).

[15] Zschiedrich, L., *Transparent boundary conditions for Maxwells equations*, PhD thesis, PhD thesis, Freie Universität Berlin (2009).